Author Manuscript

Author Manuscript

Author Manuscript

Author Manuscript

HHS Public Access

Author manuscript

Pharm Res. Author manuscript; available in PMC 2016 July 01.

Published in final edited form as:

Pharm Res. 2015 July ; 32(7): 2280–2291. doi:10.1007/s11095-015-1619-0.

Controlled endolysosomal release of agents by pH-responsive polymer blend particles

Xi Zhan[1], **Kenny K. Tran**[2], **Liguo Wang**[1], and **Hong Shen**[3,*]

[1]Department of Biological Structure, University of Washington School of Medicine, Seattle, WA 98195

[2]Department of Chemical Engineering, University of Washington School of Medicine, Seattle, WA 98195, Current address: Biogen Idec, 14 Cambridge Center, Cambridge, MA 02142

[3]Elsa Biologics, LLC, Box 25725, Seattle, WA 98165

Abstract

Purpose—A key step of delivering extracellular agents to its intracellular target is to escape from endosomal/lysosomal compartments, while minimizing the release of digestive enzymes that may compromise cellular functions. In this study, we examined the intracellular distribution of both fluorecent cargoes and enzymes by a particle delivery platform made from the controlled blending of poly (lactic-co-glycolic acid) (PLGA) and a random pH-sensitive copolymer.

Methods—We utilized both microscopic and biochemical methods to semi-quantitatively assess how the composition of blend particles affects the level of endosomal escape of cargos of various sizes and enzymes into the cytosolic space.

Results—We demonstrated that these polymeric particles enabled the controlled delivery of cargos into the cytosolic space that was more dependent on the cargo size and less on the composition of blend particles. Blend particles did not induce the rupture of endosomal/lysosomal compartments and released less than 20% of endosomal/lysosomal enzymes.

Conclusions—This study provides insight into understanding the efficacy and safety of a delivery system for intracellular delivery of biologics and drugs. Blend particles offer a potential platform to target intracellular compartments while potentially minimizing cellular toxicity.

Keywords

intracellular trafficking; pH-responsive delivery carriers; drug delivery

1. Introduction

Delivering drugs or biologics to intracellular compartments represent a promising strategy to target different signaling pathways, to alter biological activities (i.e. proliferation, differentiation), and to mediate functions of cells. The endolysosomal pathway has been the main route exploited to introduce drugs (such as cancer therapeutic drugs) and biologics

*To whom correspondence should be addressed: hong.shen@elsa-biologics.com.

Author Manuscript Author Manuscript Author Manuscript Author Manuscript

(such as nucleic acids, peptides and proteins) into cells (1–3). Anticancer drugs have to be transported to the cytoplasm (4) or other organelles (e.g. mitochondria (5)) in order to exert their therapeutic actions. Nucleic-acid-based biologics consist of DNA (6), siRNA (7) and oligoneucleotides (ODNs) (8), each with their own intracellular target. DNA has to be routed into the nucleus to be transcribed, and siRNA has to be targeted into the cytosol compartment to form RNA-induced silencing complexes (RISCs) and silence the targeted mRNA. Antigenic proteins, components of vaccines, have to be processed by proteasomes in endolysosomes or the cytosol before loading onto major histocompatibility complex class I and II molecules for priming T cells (9).

Numerous delivery systems, including viral and synthetic ones, have been developed to route drugs and biologics to the target intracellular locations. Synthetic delivery systems have garnered increasing attention due to their controllability and safety compared to many viral vectors (10). A primary function of many synthetic carriers that utilize the endolysosomal pathway is to mediate the endosomal/lysosomal escape of drugs and biologics. Endosomal/lysosomal compartments are natural processing units that cells use to degrade nutrients and to neutralize harmful materials (11). They contain a range of disgestive enzymes that are dedicated to dismantling and recycling cellular components. The inadvertent release of these enzymes could lead to detrimental effects on normal cellular functions and cause cell death (12). Some current carriers are designed to induce complete rupture (13), but may only induce the leakage of endosomal/lysosomal compartments (1, 14, 15). Nevertheless, for each carrier, it is critical to assess two aspects that determine efficiency and safety: first, can a carrier induce the release of molecules with different sizes (representing different biologics) into cytosolic compartments? Second, to what degree does one carrier lead to the release of degradative enzymes in endosomal compartments into cytosolic compartments, which may compromise cellular function?

Previously, we have developed a carrier based on polymer blend particles that can route delivered antigens to multiple intracellular compartments including endosomal/lysosomes and the cytosol by using a single model cargo, ovalbumin (16). The blend particles were made from the mixture of two polymers, a pH-irresponsive polymer (i.e. poly (lactic-co-glycolic acid) (PLGA)) and a pH-responsive copolymer that consists of 2-Propylacrylic acid (PAA), butyl methacrylate (BMA) and 2-(dimethylamino)ethyl methacrylate (DMAEMA). In this study, by using blend particles as model system, we investigated how the composition of the carrier affects the endosomal/lysosomal escape of cargos and endosomal/lysosomal enzymes with different sizes by both microscopic and biochemical analyses. These results can give us insights into tuning the composition of blend particles with respective individual therapuetic agents in order to maximize the efficacy and minimize cytotoxicity.

2. Materials and methods

2.1. Materials

Potassium hydroxide (KOH), formaldehyde (37% aqueous formaldehyde solution), anhydrous methanol and concentrated sulfuric acid were purchased from Mallinckrodt Baker Inc., NJ. Tetrahydrofuran, dichloromethane and magnesium sulfate were supplied by

Author Manuscript Author Manuscript Author Manuscript Author Manuscript

EMD Chemicals Inc., NJ. Diethyl propylmalonate, diethylamine, diethyl ether, Nhydroxysuccinimide, N,N'-dicyclohexylcarbodiimide, butyl methacrylate, 2-(dimethylamino)ethyl methacrylate, 2,2'-azobis (2-methylpropionitrile), poly (vinyl alcohol), paraformaldehyde and different molecular weights of fluorescein-labeled (FITC)-dextran were purchased from Sigma-Aldrich. Poly (lactic-co-glycolic acid) (PLGA, 50:50, IV=0.55~0.75dL/g) was from LACTEL (DURECT Corporation, AL). Calcein was purchased from MP Biomedicals, LLC. FluoSpheres® Carboxylate-Modified Microspheres (200nm, Dark Red Fluorescent) and all cell culture reagents were from Life Technologies, NY. Acridine orange was purchased from AnaSpec Inc, San Jose, CA. Digitonin was purchased from Santa Cruz Biotechnology, Inc (TX).

2.2. Cell Culture

DC2.4 cells were cultured in Roswell Park Memorial Institute (RPMI) 1640 medium, supplemented with 10% fetal bovine serum (FBS), 1% penicillin-streptomycin (P-S), 1% L-glutamine, 1% HEPES and 50μM 2-mercaptoethanol. The cells were maintained in an incubator at 37 °C and 5% CO_2.

2.3. Synthesis of tri-polymer

2-Propylacrylic acid (PAA) monomer that was utilized for the following polymerization was synthesized based on a previous report by Ferritto and Tirell (17). Briefly, KOH (1M) in enthanol (95% aqueous solution) was added into diethyl propylmalonate (9.2g, 0.0455mol), and allowed to stir for overnight (> 12 h) at room temperature. After acidification with HCl (1M) to pH 2, the mixture was extracted three times by diethyl ether. Then the crude product was cooled to − 4 °C prior to the addition of diethylamine (4.5 ml, 3.2 g) and formaldehyde solution (3.25 ml, 3.54 g, 37% aqueous solution). The solution was warmed to room temperature and stirred for 24 h, followed by another 8 h stirring at 60 °C with reflux. After being cooled to 0 °C, the concentrated sulfuric acid was added drop-wise under stirring until no bubbles appeared. Diethyl ether was utilized to extract product three times and then removed by rotary evaporator. 1M KOH aqueous solution was added into the crude product from the last step, and heated to 85 °C for 20 h with reflux. After acidification with 1M HCl to pH 2, the crude PAA was extracted by diethyl ether and then isolated by rotary evaporation. Pure PAA product was obtained by vacuum-distillation and determined by nuclear magnetic resonance (NMR) spectroscopy (500 MHz ^{1}H Bruker spectrometers).

The free radical polymerization of 2-Propylacrylic acid (PAA), butyl methacrylate (BMA), 2-(dimethylamino)ethyl methacrylate (DMAEMA) was adapted from a procedure reported previously (18). PAA, BMA and DMAEMA were vacuum distilled before use. Briefly, the reaction mixture of monomers (PAA:DMAEMA:BMA =1:1:2 (mole ratio)) and 2,2'-azobis (2-methylpropionitrile) (AIBN, 2 mM) was mixed in tetrahydrofuran (THF). The polymerization was carried out at 60 °C for 15 h under a stream of nitrogen. The solution was then poured into an excess amount of diethyl ether and pentane, and washed twice with 40 ml ice-cold pentane. The precipitated polymer was collected and dried under vacuum. Molecular weight of polymer was determined by gel permeation chromatography (GPC, Malvern Instruments Ltd). Weight average molecular weight (Mw) and number average molecular weight (Mn) were calculated in reference to poly (methyl methacrylate)

Author Manuscript Author Manuscript Author Manuscript Author Manuscript

standards. The compositions of the tri-polymers were determined by ^{1}H NMR measurements (500 MHz 1H Bruker spectrometers) in $CDCl_3$.

2.4. Synthesis of HiLyte647-labeled PLGA

0.2 g carboxylated PLGA was dissolved in 1 ml of DCM overnight. Five times molar excess of N-Hydroxysuccinimide (NHS) and dicyclohexylcarbodiimide (DCC) were dissolved in 1 ml of DCM and added to the PLGA solution. The reaction solution was incubated at room temperature on a shaker. After 24 hours, the polymer was precipitated by adding 40 ml of ice-cold anhydrous methanol and washed twice with 20 ml methanol. The activated PLGA was collected and freeze-dried overnight.

0.2 g of activated PLGA polymer was dissolved in 1ml of DCM. 10 mg/ml HiLyte647 (AnaSpec Inc., Fremont, CA) in 100 μl DMSO and 10 × molar excess N,N-Diisopropylethylamine (DIEA) were added into PLGA solution. After 24 h reaction at room temperature on a shaker, the HiLyte647-labeled PLGA was precipitated by adding 60 ml ice-cold methanol drop-wise. The conjugated polymer was washed 3 times with ice-cold diethyl ether and freeze-dried overnight.

2.5. Fabrication and characterization of blend particles

A double-emulsion method was used to fabricate the blend particles from the tripolymer and PLGA. The tri-polymer and PLGA were dissolved in 1 ml DCM with different weight ratios (tri-polymer in total polymer weight, 0, 0.1, 0.2, 0.5) overnight. 10 wt% HiLyte647-labeled PLGA was also spiked into the mixture of the polymers in order to label particles. 100 μl of DPBS was added to the polymer mixture drop-wise. 2 ml of 5% PVA was then added drop-wise into the polymer solution while vortexing, and the solution was sonicated twice, 10 s each time with a brief pause between. The emulsion was added into 4 ml of 5% PVA under stirring and followed by sonication. Then the emulsion was poured into 4 ml 0.06% of PVA solution under stirring. The final emulsion was stirred for 3 ~ 4 h to evaporate DCM. The particles were washed 3 times with mili-Q water. Particle composition was determined by ^{1}HNMR. Particle size and zeta potential were characterized in 10 mM KNO_3 solution by dynamic light scattering (DLS) (Zetasizer Nano ZS, Malvern Instruments, MA). Scanning electron microscope (FEI Sirion SEM, FEI Company, OR) was utilized for the characterization of size and morphology.

2.6. Assessment of endosomal/lysosomal release of acridine orange (AO)

Cells were plated at a density of 2×10^5 per well in 24-well polystyrene plates and incubated overnight. Fluorescent blend particles were added at varied concentration (5, 10, 20, 50, 100 μg/ml) in fresh media, and the cells were incubated for 4 h at 37°C. For the kinetics study, fluorescent blend particles were added at 50 μg/ml concentration in fresh media. Cells were further incubated for 30 min, 2 h or 4 h at 37°C. Then the media was discarded and replaced with 2.5 μM AO in RPMI media. The cells were incubated in 37°C incubator for an additional 15 min and washed 3 × with DPBS. Cells were incubated for 30 min at 4°C in DPBS containing Fixable Viability Dye eFluor780 (1 μl in 1 ml DPBS, eBioscience). Amine-end polystyrene (200nm, PS-NH2), dark red carboxylate-modified polystyrene beads (200 nm, PS-COOH) were used as controls. The cell viability, uptake of

Author Manuscript Author Manuscript Author Manuscript Author Manuscript

particles and AO at 640 nm were immediately analyzed by flow cytometry (FACScanto, BD), and quantified by determining the geometric mean of fluorescence using Flowjo. The fluorescence of particles at different concentrations was quantified by SpectraMax (Molecular Devices) and a standard curve (fluorescence intensity versus weight concentration) was constructed for each particle type. The uptake of blend particles (geometric mean fluorescence) measured by flow cytometry was then corrected with the standard curve, and presented as weight of particle in each cell (mg/cell).

2.7. Co-delivery of different molecular weight of cargos and blend particles

DC2.4 cells were plated at 1.5×10^5 cells per well onto 12 mm-coverslips in 24-well polystyrene plates and incubated at 37°C overnight. HiLyte647-labeled blend particles were added to cells at the amount in order to achieve the same amount of intracellular particle level together with calcein (0.2 mg/ml) or FITC-dextran (2 mg/ml) of different molecular weights. Cells were incubated with particles for 4 h at 37°C. Dark-red PS-COOH particles (200nm) were used as controls. Then the coverslips were washed, and fixed with 4% paraformaldehyde in DPBS for 20 min at room temperature. The coverslips were then washed and mounted onto glass coverslips with hard-set mounting medium with DAPI (4', 6-diamidino-2-phenylindole, Vector Laboratories Inc., CA). Cells were imaged by the confocal microscope (LSM 510 Meta, Zeiss, 63 × oil immersion objective). Each z section is 0.8 μm in thickness. The colocalization of blend particles and fluorecent cargos was analyzed using ImageJ software and JACoP plugin. A background region of each image was selected first, and the threshold was set that gave zero overlap coefficient (Manders' coefficient) between particle and cargo channels. Then the images of 15 cells for each group were chosen and Manders' coefficient of fluorecent cargo (G) was utilized to evaluate the overlap of particles and different molecualar weight cargos.

$$M = \frac{\sum_i G_{i,coloc}}{\sum_i G_i}$$

2.8. Co-localization of endosomal/lysosomal compartment and particles

DC2.4 cells were plated as previously described. HiLyte647-labeled blend particles were added at a concentration of 50 μg/ml and incubated for 4 h at 37°C. Dark-red PS-COOH particles (200 nm) were used as controls. After being fixed with 4% paraformaldehyde in DPBS for 20 min at room temperature, the cells were washed twice with blocking buffer (1% FBS in DPBS) and then incubated with blocking buffer for another 1.5 h. Then, 250 μl rat anti-mouse LAMP-2 (2 μg/ml in blocking buffer, Abcam Inc., MA) was added to the cells. After being incubated at 4°C for 1 h, the antibody solution was removed and the cells were washed twice with the blocking buffer. A secondary antibody, donkey anti-rat-Alexa 488, was added at a concentration of 2 μg/ml in blocking buffer (250 μl/well) and incubated at 4°C for an additional 1 h. The coverslips were then washed and mounted onto glass coverslips with hard-set mounting medium with DAPI (Vector Laboratories Inc., CA). Confocal microscope was utilized to assess the colocalization of particles with LAMP-2 as previous described and ImageJ was used to analyze the images.

Author Manuscript Author Manuscript Author Manuscript Author Manuscript

2.9. Measurement of the release of endosomal/lysosomal enzymes by using digitonin to selectively permeabilize cell membranes

Cell permeablization with digitonin-containing buffer was developed based on previous reports (19, 20). Initially, the digitonin concentration and treatment time were optimized. DC2.4 cells (4×10^6 cells/ml) in 15 ml-centrifuge tubes were treated with the digitoni-containing buffer (20, 30 or 40 μg/ml digitonin diluted from 20 mg/ml digitonin/DMSO stock, 250 mM sucrose, 20 mM Hepes, 10 mM KCl, 1.5 mM $MgCl_2$, 1 mM EDTA, 1 mM EGTA, pH 7.4) on ice for 5, 10 or 20 min. The permeabilized cells were processed, and enzyme activities released into cytosol were measured as below. Cells lysed with lysis buffer provided in the enzyme assay kits were used as positive controls.

DC2.4 cells were plated at 2×10^6 cells per well in 6-well polystyrene plates and incubated at 37°C for 1.5 ~ 2 h. HiLyte647-labeled blend particles or control particles were added at an amount to yield an equivalent amount of intracellular level (50 μg/ml of blend 0.1 particles, and we used different concentrations of other type of particles to achieve the same intracellular level of blend 0.1 particles), and incubated for 4 h at 37°C. Cells in two wells were then trypsinized and combined into one 15 ml-centrifuge tube (~4×10^6 cells/tube). Cells were washed 5× with ice-cold DPBS. It is critical to thoroughly wash cells to remove traces of trypsin, which may affect the assay of enzyme activities. Cells were then resuspended in 0.5 ml of digitonin extraction buffer containing optimized digitonin concentration and incubated for the optimal duration on ice. 10 μl of each cell suspensions was taken after incubation and stained with 0.02% trypan blue. The number and fraction of permeabilized cells were counted. The rest of cell suspensions were centrifuged at 1000 × g at 4°C for 10 min. The supernatant was collected and then further centrifuged at 20000 × g at 4°C for 30 min. After the last centrifuge, 0.2 ml supernatant was taken for assessing the enzyme activities. The activity of β-N-Acetylglucosaminidase, a lysosomal enzyme, was measured by following the instruction of β-N-Acetylglucosaminidase Assay Kit (Sigma-Aldrich, MO), and expressed as Unit / 10^5 permeabilized cells.

2.10. Statistical Analysis

Student's t test was used to compare two experimental groups when needed. P value < 0.05 was considered to be statistically significant. All the experiments were repeated two to four times independently.

3. Results

3.1. Synthesis of pH-sensitive copolymer

The pH-sensitive copolymer consisting of PAA, BMA and DMAEMA was chosen for fabricating blend particles. The monomers of PAA and DMAEMA have pKa of 6.7 and 8.3, respectively (21, 22). They undergo conformational changes at endosomal pH (acidic pH) and have been used to deliver agents into cytosolic compartments (2, 18). Recently, the copolymer consisting of both PAA and DMAEMA has been synthesized for the delivery of siRNA (23). It has been suggested that the inclusion of both PAA and DMAEMA can finely tune the pH responsiveness (18). The addition of BMA increases the hydrophobicity of copolymers, which may facilitate the blending of the copolymer with PLGA for the

Author Manuscript Author Manuscript Author Manuscript Author Manuscript

formation of blend particles (24).The monomer PAA was first synthesized and vacuum-distilled, and a yield of 58.8% was achieved. The pH-sensitive copolymer, called the tri-polymer hereafter, was subsequently synthesized by free radical polymerization. The molar ratio of monomers in feed was 1:1:2 (PAA : DMAEMA : BMA). Based on nuclear magnetic resonance (NMR) analysis (Fig S1b), the molar ratio of the three units in the tri-polymer was 1.5:1:2.5. The weight average molecular weight (MW) was determined by gel permeation chromatography (GPC), and had Mw of ~ 22 kDa, and PDI of 1.2.

3.2 Characterization of blend particles

The two polymers were successfully blended and formed into particles with the double-emulsion solvent evaporation fabrication process. The composition of the tri-polymer and PLGA in blend particles was determined by NMR. The ratio of the two polymers in the blend particles remained nearly the same as the initial feed ratio (Table 1, Fig S2). Different types of blend particles are named based on the weight ratio of the tri-polymer as blend 0, 0.1, 0.2, and 0.5.

The size of particles was characterized by both DLS and SEM. The measurements by DLS showed that the hydrodynamic diameter of blend particles had a range from 250 nm to 450 nm (Fig 1a). The blend 0.1 and blend 0.2 exhibited the similar size to blend 0 particles while the blend 0.5 particles were relatively larger compared to other particles. The hydrodynamic diameter of all the particles did not change significantly when the pH varied between 2.0 and 7.0 (Fig 1a). At pH 9–10, agglomeration was observed for both blend 0.2 and blend 0.5 particles. When the pH approached 11.0, particles returned to a mono-dispersed population. The measurements by SEM showed that all types of the particles had diameters between 150 nm and 200 nm in a dry state (Fig 2, Table 2), which were smaller compare to the hydrodynamic diameters determined by DLS. Particles exhibited a larger hydrodynamic diameter as measured by DLS due to the charged and flexible side chains present on the tripolymer while in solution. In contrast, for SEM images, the samples were dried and imaged in a dry state, which yielded smaller diameters compared to hydrodynamic diameters.

The particle surface charge at different pHs, characterized by zeta potential, was measured by DLS (Fig 1b). Blend 0 particles had a neutral zeta potential while the three types of blend particles had strong positive charge (~30 mV) at the acidic pH. The positive charge was attributed to the protonation of amine group of DMAEMA. The zeta potential of blend particles was near neutral at the pH of 10.0 and became negative at the pH of 11.0 (Fig 1b, Table 2), which was due to the de-protonation of the carboxyl group of PAA. The change of zeta potential explains the switch of mono-dispersity to agglomeration and then to monodispersity again when the pH changed from 2.0 to 11.0. It also indicates that the tri-polymer was at least partially displayed on the surface of particles.

3.3 Blend particles can induce endosomal/lysosomal leakage

We first tested whether blend particles were capable of inducing the endosomal/lysosomal leakage by using acridine orange (AO). AO is a lysosomotropic dye, and has been previously used to determine endosomal or lysosomal leakage (25). As a weak base, the

Author Manuscript Author Manuscript Author Manuscript Author Manuscript

unprotonated form of AO is permeable to cell and organelle membranes. Once inside acidic compartment such as endosomes/lysosomes, the dye becomes protonated, entrapped, and accumulates in the endosomes/lysosomes as dimers, trimers or oligomers (26). Dimers, trimers or oligomers of AO exhibit red emission at 640 nm while monomers show green emission at 525 nm. Thus, the fluorescent intensity of AO at 640 nm can be used to examine the integrity of endosomal/lysosomal compartments since the endosomal/lysosomal leakage results in the decrease of AO signal at 640 nm.

The endosomal/lysosomal leakage mediated by blend particles of different ratios was examined at varying incubation times (30 min, 2 h, 4 h). Polystyrene (PS) particles, which do not induce appreciable endosomal/lysosomal escape (27), were used as controls. As shown in Fig 3a, no significant decrease of AO intensity was observed for both blend and PS particles after 30 min incubation. After 2 and 4 h, cells containing blend 0.1, 0.2 and 0.5 particles exhibited reduced AO intensity at 640 nm. In contrast, the AO intensity remained constant in cells exposed to PS particles with either amine (PS-NH2) and carboxylated (PS-COOH) surface chemistry. We also examined the cell viability and integrity of cell membrane by using the Fixable Viability Dye eFluor780 (ebioscience) (Fig S3). Blend particles did not compromise the integrity of cell membrane at the concentrations under 50 μg/ml. Therefore, the reduction of AO intensity at 640 nm was not due to the release of AO into the extracellular space through the cell membrane. These results indicate that blend particles were able to induce the endosomal/lysosomal leakage of cargos.

The AO intensity at different levels of uptake of blend particles was subsequently evaluated by flow cytometry (Fig 3b,c). PLGA was labeled with HiLyte647 and doped in each type of particles to monitor the uptake of particles. The geometric mean fluorescence of HiLyte647 was used to indicate the level of uptake. The fluorescence of particles was also measured at varying weight concentrations by a fluorometer, and then was utilized to correct the geometric mean fluorescent intensity of HiLyte647 determined by flow cytometry. The error of uptake caused by the difference in the fluorescence intensity of single particle between different particle types was thus minimized. AO intensity of cells exposed to different types of particle was plotted with the level of uptake (Fig 3b,c). Compared to PS particles, all of three kinds of particles showed a decreasing trend in AO intensity with increasing particle uptake as expected.

3.4. The release of cargos with different molecular weights from endosomal/lysosomal to cytosolic compartments mediated by blend particles

AO is a small molecule with a MW of 265.35 Da. Different blend particle exhibited similar abilities of inducing the endosomal/lysosomal leakage of AO. Drugs and biologics used as therapeutics or targeting signaling pathways possess varying sizes. For instance, small drugs, such as doxorubicin, are of a few hundreds of daltons (15), while oligonucleotides, peptide and siRNA have MWs ranging from a few kDa to 20 kDa (3, 8, 28, 29). The MW of macromolecules such as some proteins or plasmid DNA is more than one million daltons (1, 30). We subsequently examined the intracellular distribution of cargos with different molecular weights mediated by blend particles utilizing confocal microscopic analysis (Fig 4a). In order to achieve equivalent particle uptake with different particle types, varying

Author Manuscript Author Manuscript Author Manuscript Author Manuscript

amounts of each particle type was delivered to cells based on the dependence of uptake on the concentration of particles.

Fluorescent molecules with varying molecular weights (calcein, FITC-dextran with the MW of 4, 40, 150, and 2000 kDa) were co-delivered with particles. Calcein and fluorescent dextran have been used as tracers to monitor the stability of endosomal/lysosomal compartments because they are membrane-impermeable molecules (1, 13, 14). These molecules are taken up by fluid phase pinocytosis (31) and are able to fuse into particle containing endosomal/lysosomal compartments (32). For all sizes of fluorescent molecules, in the absence of particles, the endocytosed molecules appeared as punctate structures in cells, indicting they remained in distinct endosomal/lysosomal compartments (Fig 4a). In the presence of PS particles, the punctate patterns remained regardless of the size of cargos, indicating little endosomal/lysosomal leakage occurred. In the presence of all the blend particles, for molecules of low MWs such as calcein (MW=622.55Da), FITC-dextran with a MW of 4 k and 40 kDa, cells exhibited a diffuse pattern of fluorescence, indicating endosomal/lysosomal leakage; for 150 k and 2000 k Da of dextran, cells displayed the punctate patterns.

We then calculated co-localization coefficients (Manders' coefficients) of particles and cargos (Fig 4b). For all molecular weights of FITC-dextran, blend particles resulted in lower degree of overlap compared to PS particle controls. This suggests that blend particles mediated the release of FITC-dextran from endo/lysosomal compartments into the cytosol, while PS particles remained co-localized with dextran. With increasing MW of FITC-dextran, there was increasing level of overlap for all blend particles, indicating lower levels of escape of dextran into the cytosolic space. For calcein and FITC-dextran MW 40 kDa, blend particles resulted in ~20% and ~40% of the level of overlap observed with control PS particles, respectively. In contrast, for FITC-dextran with 2000 kDa MW, blend particles resulted in ~70–90% of the level of overlap observed with control PS particles, indicating that very little escape occured. This suggests that blend particles mediate endosomal escape of cargos in a cargo size-dependent manner. Interestingly, the degree of overlap was also dependent on the composition of blend particles for larger size of FITC-dextran; 0.1 blend particles exhibited statistically less overlap than 0.2 and 0.5 blend particles. We attempted further quantification of the release of cargos into cytosolic space by separating the cytosol from endolysosomal compartments using cell fractionation. However, the artifacts caused during the fractionation complicated the quantification.

We also confirmed whether blend particles remained in endosomal/lysosomal compartments. Blend particles remained inside endosomal/lysosomal compartments labeled by LAMP-2, similar to PS particles (Fig S4). These results indicated that blend particles did not lead to complete rupture of endosomal/lysosomal compartments and escape into cytosolic space.

3.5. Semi-quantification of the release of endosomal/lysosomal enzymes into cytosolic compartments

Digitonin, known as a cholesterol-complex-forming agents, has been utilized to selectively permeabilize cells in the studies of nuclear import (33), mitochondrial isolation (19) and

Author Manuscript Author Manuscript Author Manuscript Author Manuscript

roles of lysosomal enzymes in apoptosis of cells (20). Cholesterol is abundant in cell plasma membrane (~0.5 mol cholesterol per mol phospholipid) while it is 5 to 17 times less abudant in organelle membrane (0.03–0.08 mol cholesterol per mol phospholipid) (34). We then developed a method to examine the release of endosomal/lysosomal enzymes into the cytosolic space by using digitonin-containing buffer to permeablize the cell membrane and to extract contents from the cytosolic compartment while maintaining the integrity of intracellular organelles.

The digitonin concentration and treatment duration were first optimized as shown in Fig S5. N-acetyl-β-D-glucosaminidase (NAG) (140 kDa), a representative lysosomal enzyme, was used to evaluate the integrity of endosomal/lysosomal organelles (35). With the lower concentration (20 μg/ml) of digitonin, less than 40% cells were permeabilized for all three treatment durations (5, 10, 20 min), while the highest concentration (40 μg/ml) induced 100% cell permeabilization within 5 min. The digitonin-treated group exhibited similar enzyme activities as untreated cells. Compared to the group treated with lysis buffer, which was expected to release all the endosomal/lysosomal enzymes, the digitonin treated group resulted in about 10 times lower activity of both enzymes (Fig S5). These results confirmed that the digitonin buffer was able to permeabilize the cell membranes without completely disrupting endosomal/lysosomal compartments, which is consistent with previous study (20). For subsequent studies, 30 μg/ml of digitonin and 10 min treatment time were chosen.

Subsequently, we assessed the release of NAG induced by blend particles. PS particles were used as controls. Digitonin buffer successfully permeabilized cells with all types of particles (Fig 5a). Blend particles caused the release of 20% of total endosomal/lysosomal NAG while PS particles did not cause any significant level of release of enzymes (Fig 5b). There was no clear trend for blend particles with different tri-polymer compositions.

4. Discussion

In this study, we used blend particles as model intracellular delivery systems to examine the escape of molecules with different molecular weights and endosomal/lysosomal enzymes into cytosolic compartments. Blend particles consisted of a random pH-responsive copolymer (tri-polymer), poly (BMA-co-PAA-co-DMAEMA) and PLGA. PLGA here not only acted as a hydrophobic core that facilitated the formation of particles, but also minimized the pH-dependent swelling of the particles (Fig 1a). The ratio of tri-polymer to PLGA was varied between 0 to 0.5 in order to tune the ability of blend particles in sequestering protons (Fig 1b). In this study, the composition of the tri-polymer was fixed. Potentially, it can be further tuned by adjusting the composition of three monomers, BMA, PAA and DMAEMA in the tri-polymer. We demonstrated that blend particles enabled the release of agents with the MW ranging from a few hundred to 40 k daltons into the cytosolic space. They did not induce the complete rupture of endosomal/lysosomal compartments and released about 20% of total endosomal/lysosomal NAG (MW 140kDa) into the cytosolic space (Fig S4, Fig 5).

Three different methods were used in this study to evaluate the endosomal/lysosomal escape of cargos induced by blend particles. AO is a cationic dye which exhibits fluorescence

Author Manuscript Author Manuscript Author Manuscript Author Manuscript

emission shifts at different pHs. All the blend particles induced the reduction of AO intensity at 640 nm, indicating the release of AO from endosomal/lysosomal compartments (Fig 3). Using flow cytometry only provided the change of fluorescence intensity for the whole cell population and not the intracellular distribution of cargos for individual cells. This method cannot provide the information on how the intracellular distribution of cargos depended on the size of cargos and the composition of carriers. Thus, confocal microscopy was also utilized to evaluate the endosomal/lysosomal release of cargos with different sizes into cytosolic space induced by blend particles.

Calcein and different molecular weight of FITC-dextrans were co-delivered to DC2.4 cells with blend particles. We demonstrated that blend particles did not induce the complete rupture of endosomal/lysosomal compartments (Fig S4); all the blend particles exhibited the cargo size-dependent intracellular distribution. A number of factors may result in biased assessment of the size of cargos escaping into the cytosolic space by confocal microscopic analysis. One is the degradation of dextran molecules and the dissociation of FITC molecules within the endosomal/lysosomal compartments. Since there was no appreciable level of fluorescence in cytosolic space for FITC-dextran with MWs of 150 kDa or higher, the degradation was not expected to be significant. Second, calcein and dextran molecules themselves may cause the osmotic pressure change of endolysosomal compartments, leading to rupture. The control groups (PS particles and without particles) did not exhibit detectable levels of cytosolic fluorescence, which showed that the effect of calcein and dextran molecules themselves were negligible. An additional factor may be the fluorescence and diffusion property of dextran molecules. Higher molecular weights of dextran have lower diffusion coefficients (36), which may lead to slower diffusion throughout the cytosolic space and remained near endosomal/lysosomal compartments during the duration of experiments. Given the lateral resolution of confocal images (greater than 200 nm), these molecules might seem to be punctated and appear to remain inside the endolysosomal compartments. We calculated the diffusion length of dextran molecules used in this study. The experimental duration (4 h) was sufficient for FITC-dextran of 2,000 k Daltons to migrate several micrometers. Therefore, the diffusion limitation within a cytosolic space is not expected to result in the punctated distribution pattern.

Confocal microscopic images provided an intuitive grasp of the distribution of cargos among the cytosolic space and endosomal/lysosomal compartments. We also quantified the distribution by computing co-localization coefficients of particles and cargos (Fig 4b). The results suggest that blend particles mediate endosomal escape of cargos dependent on both cargo size and the composition of blend particles. In our confocal micropic analysis, we noticed that not all of soluble calcein/FITC-dextran molecules were co-localized with particles in DC2.4 cells for both blend and PS particles. This could be due to the size-selective movement or segreation within the endocytic compartments (31). This size segreation occurs dynamically. Some of cargos may be sorted into different endocytic compartments from particles initially and would remain in the endocytic compartments. Since the size of different blend particles and PS particles was similar, we expect the level of FITC-dextran that did not intially overlap with particles to be simlar for PS and different blend particles. Though the co-localization coefficients may not give us the accurate estimation of release of cargos into cytosol mediated by each particle type, they permited us

Author Manuscript Author Manuscript Author Manuscript Author Manuscript

compare different particles semi-quantitatively. We tried to separate two compartments by cell fractionation. Only 20 ~ 50% of cells were ruptured while preserving the integrity of endolysosomal membranes. A more accurate and quantitative method is needed to analyze the intracellular distribution of cargos.

Endosomal/lysosomal compartments contain various types of enzymes, such as nucleases, proteases, carbohydrate and lipid digesting enzymes (11) (Table S1). Those enzymes could damage cells when released to the cytosol (37). We assessed the release of two representative enzymes, Cathepsin B (~25 kDa) and N-acetyl-β-D-glucosaminidase (NAG, ~140 kDa), into cytosolic compartments by "extracting" the cytosolic components using digitonin-containing buffers. However, the enzyme activity of Cathepsin B was inconsistent and influenced by any trace of trypsin used to detach the cells. Therefore, we only used NAG to assess the release of enzymes into cytosolic space. This method not only provided us information on the release of enzymes but also the escape of cargos of different MWs into the cytosolic compartments induced by carriers. Blend particles only induced a small fraction release of NAG enzymes, which corresponded with confocal analysis of FITC-dextrans of varying MWs (Fig 4). We were not able to obtain an assay kit to examine enzymes greater than 140 kDa. Based on our studies on the release of cargos of varying MWs (Fig 4), we do not expect that a significant level of enzymes greater than 150 kDa to be released into cytosolic compartments.

Two possible mechanisms have been proposed for the delivery of cargos into the cytosolic space mediated by pH-sensitive particles containing components of PAA, BMA or DMAEMA. Hu *et al*. reported a core-shell particle system containing DMAEMA. The diameter of these particles doubled in endolysosomal environments compared to that in the extracellular environment (13). The increase in diameter led to a quadruple increase of surface area that required much more lipids to maintain the stable endolysosomal structures, leading to particle escape into the cytosolic space. In our case, in the pH range of cell compartments (cytosol: pH 7.4, endosome: pH 5~6, lysosome: pH 4.6), the size of blend particles was around 400 nm for all compositions and did not change significantly when the pH changed (Fig 1b). Thus, the complete rupture of endosomal/lysosomal compartments caused by the swelling of particles was unlikely for the blend particles used in our study, which was consistent with our previous observations (38). It has also been hypothesized that BMA directly interacted with endosomal/lysosomal membranes, leading to the leakage or dissolution of endosomes and lysosomes (39). In the case of blend particles, the PLGA matrix may have restrained the conformational change of the tri-polymer, limiting the interaction of PAA or BMA with endosomal membranes.

Instead, blend particles may result in a more controlled swelling of endosomal/lysosomal compartments due to the "proton-sponge" effect. The proton-sponge effect results from the sequestration of protons by polycations. The accumulation of protons is accompanied by an increase of chloride anions and water within endosomal/lysosomal compartments in order to balance the increasing osmotic pressure (40). We propose two possible models that resulted in the release of cargos into cytosolic space. One model is what we term the "leaking-resealing" process: the swelling of endosomes/lysosomes due to the proton-sponge exceeds the surface tension of lipid molecules and results in the breaching of the membrane.

Author Manuscript Author Manuscript Author Manuscript Author Manuscript

Molecules may then escape into the cytosol through the regions where the lipid membrane is compromised. Upon the release of the osmotic pressure, the membrane reseals, and the particles, which were too big to escape from the breached regions, remain in the endosomal/lysosomal compartments. This “leaking-resealing” process may repeat several cycles as a dynamic process. Another possible model is what we term the “fission” process. The increasing osmotic pressure in endosomal/lysosomal compartments may result in the division and re-sealing of the offspring compartments. During this process, some of the fluorescent molecules may escape into cytosol or remain in one of the offspring compartments. It is also possible that these two mechanisms co-exist. Single-particle tracking techniques may enable elucidation of the detailed processes of the release of cargos by carriers.

In summary, the blend particles in this study did not completely rupture the endosomes/lysosomes. Instead, they may cause either “fission” or “leaking - resealing” of endosomes/lysosomes. The distribution of agents in two intracellular compartments, endosomes/lysosomes and cytosol, was dependent the size of cargos and the composition of blend particles. For the composition of blend particles used in this study, cargos with the size of less than 150 kDa can be readily released into the cytosolic space.

5. Conclusion

This study utilized semi-quantitative methods to assess the ability of a carrier in inducing the release of cargos and endosomal/lysosomal enzymes of different sizes into cytosolic compartments, which is critical for understanding the efficacy and safety of a drug carrier. We demonstrated that the delivery platform built upon blend particles provides more controlled release of cargos and endolysosomal enzymes. In addition, the composition of tripolymer can be tuned to obtain lower or higher capacity of blend particles in sequestering protons and thus ability of inducing endolysosomal release of cargos and endosomal/lysosomal enzymes. Further studies on correlating the sequestering protons with the release of cargos and endosomal/lysosomal enzymes into cytosolic space would provide a design framework for pH-responsive based delivery carriers.

Supplementary Material

Refer to Web version on PubMed Central for supplementary material.

Acknowledgements

The authors want to thank the Cell Analysis Facility in the Department of Immunology, the Keck Microscopy Facility, and the NanoTech User Facility (NTUF) in University of Washington. This study was funded by (AI088597) from the National Institutes of Health (NIH) and the NSF CAREER Award to H.S.

Abbreviations

PLGA	poly(lactic-co-glycolic acid)
PAA	2-Propylacrylic acid

Author Manuscript Author Manuscript Author Manuscript Author Manuscript

BMA	butyl methacrylate
DMAEMA	2-(dimethylamino)ethyl methacrylate
AIBN	2,2'-azobis(2-methylpropionitrile)
DCM	Dichloromethane
PVA	Polyvinyl alcohol
PS	Polystyrene
PS-NH2	Amine-end polystyrene particles
PS-COOH	Carboxylate-modified polystyrene particles
DPBS	Dulbecco's Phosphate Buffered Saline
AO	acridine orange
DAPI	4',6-diamidino-2-phenylindole
FITC	Fluorescein isothiocyanate
NAG	N-acetyl-β-D-glucosaminidase
NMR	nuclear magnetic resonance spectroscopy
GPC	gel permeation chromatography
DLS	dynamic light scattering
SEM	scanning electron microscope
MW	molecular weight
PDI	polydispersity index
LAMP-2	lysosomal associated membrane protein-2

References

1. Bonner DK, Leung C, Chen-Liang J, Chingozha L, Langer R, Hammond PT. Intracellular Trafficking of Polyamidoamine-Poly (ethylene glycol) Block Copolymers in DNA Delivery. Bioconjugate Chem. 2011; 22(8):1519–1525.
2. Convertine AJ, Diab C, Prieve M, Paschal A, Hoffman AS, Johnson PH, Stayton PS. pH-Responsive Polymeric Micelle Carriers for siRNA Drugs. Biomacromolecules. 2010; 11(11):2904–2911. [PubMed: 20886830]
3. Grayson ACR, Doody AM, Putnam D. Biophysical and structural characterization of polyethylenimine-mediated siRNA delivery in vitro. Pharmaceutical Research. 2006; 23(8):1868–1876. [PubMed: 16845585]
4. Soppimath KS, Liu LH, Seow WY, Liu SQ, Powell R, Chan P, Yang YY. Multifunctional core/shell nanoparticles self-assembled from pH-induced thermosensitive polymers for targeted intracellular anticancer drug delivery. Adv Funct Mater. 2007; 17(3):355–362.
5. Fernandex-Carneado J, Van Gool M, Martos V, Castel S, Prados P, de Mendoza J, Giralt E. Highly efficient, nonpeptidic oligoguanidinium vectors that selectively internalize into mitochondria. J Am Chem Soc. 2005; 127(3):869–874. [PubMed: 15656624]

Author Manuscript Author Manuscript Author Manuscript Author Manuscript

6. Wang C, Ge Q, Ting D, Nguyen D, Shen HR, Chen JZ, Eisen HN, Heller J, Langer R, Putnam D. Molecularly engineered poly (ortho ester) microspheres for enhanced delivery of DNA vaccines. Nat Mater. 2004; 3(3):190–196. [PubMed: 14991022]
7. Golzio M, Mazzolini L, Moller P, Rols MP, Teissie J. Inhibition of gene expression in mice muscle by in vivo electrically mediated siRNA delivery. Gene Ther. 2005; 12(3):246–251. [PubMed: 15592423]
8. Jewell CM, Jung JM, Atukorale PU, Carney RP, Stellacci F, Irvine DJ. Oligonucleotide Delivery by Cell-Penetrating "Striped" Nanoparticles. Angew Chem Int Edit. 2011; 50(51):12312–12315.
9. Banchereau J, Briere F, Caux C, Davoust J, Lebecque S, Liu YT, Pulendran B, Palucka K. Immunobiology of dendritic cells. Annu Rev Immunol. 2000; 18 767-+.
10. Thomas M, Klibanov AM. Non-viral gene therapy: polycation-mediated DNA delivery. Appl Microbiol Biot. 2003; 62(1):27–34.
11. Berg T, Gjoen T, Bakke O. Physiological Functions of Endosomal Proteolysis. Biochem J. 1995; 307:313–326. [PubMed: 7733863]
12. Guicciardi M, Leist M, Gores G. Lysosomes in cell death. ONCOGENE. 2004; 23(16):2881–2890. [PubMed: 15077151]
13. Hu Y, Litwin T, Nagaraja AR, Kwong B, Katz J, Watson N, Irvine DJ. Cytosolic delivery of membrane-impermeable molecules in dendritic cells using pH-Responsive core-shell nanoparticles. Nano Letters. 2007; 7(10):3056–3064. [PubMed: 17887715]
14. Morishige T, Yoshioka Y, Inakura H, Tanabe A, Yao XL, Narimatsu S, Monobe Y, Imazawa T, Tsunoda S, Tsutsumi Y, Mukai Y, Okada N, Nakagawa S. The effect of surface modification of amorphous silica particles on NLRP3 inflammasome mediated IL-1 beta production, ROS production and endosomal rupture. Biomaterials. 2010; 31(26):6833–6842. [PubMed: 20561679]
15. Cheng ZL, Chen AK, Lee HY, Tsourkas A. Examination of Folate-Targeted Liposomes with Encapsulated Poly (2-propylacrylic acid) as a pH-Responsive Nanoplatform for Cytosolic Drug Delivery. Small. 2010; 6(13):1398–1401. [PubMed: 20564486]
16. Tran KK, Zhan X, Shen H. Polymer Blend Particles with Defined Compositions for Targeting Antigen to Both Class I and II Antigen Presentation Pathways. Advanced Healthcare Materials. 2014; 3(5):690–702. [PubMed: 24124123]
17. Ferrito MTD. Poly (2-ethylacrylic acid). Macromol Synth. 1992; 11:59–62.
18. Takeda N, Nakamura E, Yokoyama M, Okano T. Temperature-responsive polymeric carriers incorporating hydrophobic monomers for effective transfection in small doses. J Control Release. 2004; 95(2):343–355. [PubMed: 14980782]
19. Kuznetsov AV, Veksler V, Gellerich FN, Saks V, Margreiter R, Kunz WS. Analysis of mitochondrial function in situ in permeabilized muscle fibers, tissues and cells. Nat Protoc. 2008; 3(6):965–976. [PubMed: 18536644]
20. Foghsgaard L, Wissing D, Mauch D, Lademann U, Bastholm L, Boes M, Elling F, Leist M, Jaattela M. Cathepsin B acts as a dominant execution protease in tumor cell apoptosis induced by tumor necrosis factor. Journal of Cell Biology. 2001; 153(5):999–1009. [PubMed: 11381085]
21. Grainger, SJE-SMEH. Biologically-Responsive Hybrid Biomaterials. Singapore: World Scientific Publishing; 2010. Stimuli-Sensitive Particles for Drug Delivery.
22. van de Wetering P, Moret EE, Schuurmans-Nieuwenbroek NME, van Steenbergen MJ, Hennink WE. Structure-activity relationships of water-soluble cationic methacrylate/methacrylamide polymers for nonviral gene delivery. Bioconjugate Chem. 1999; 10(4):589–597.
23. Convertine AJ, Benoit DSW, Duvall CL, Hoffman AS, Stayton PS. Development of a novel endosomolytic diblock copolymer for siRNA delivery. J Control Release. 2009; 133(3):221–229. [PubMed: 18973780]
24. Kurisawa M, Yokoyama M, Okano T. Transfection efficiency increases by incorporating hydrophobic monomer units into polymeric gene carriers. J Control Release. 2000; 68(1):1–8. [PubMed: 10884574]
25. Xia T, Kovochich M, Liong M, Zink JI, Nel AE. Cationic polystyrene nanosphere toxicity depends on cell-specific endocytic and mitochondrial injury pathways. Acs Nano. 2008; 2(1):85–96. [PubMed: 19206551]

Author Manuscript Author Manuscript Author Manuscript Author Manuscript

26. Palmgren MG. Acridine - orange as a probe for measuring pH gradients across membranes - mechanism and limitations. Anal Biochem. 1991; 192(2):316–321. [PubMed: 1827963]
27. Shen H, Ackerman AL, Cody V, Giodini A, Hinson ER, Cresswell P, Edelson RL, Saltzman WM, Hanlon DJ. Enhanced and prolonged cross-presentation following endosomal escape of exogenous antigens encapsulated in biodegradable nanoparticles. Immunology. 2006; 117(1):78–88. [PubMed: 16423043]
28. Lin YL, Jiang GH, Birrell LK, El-Sayed MEH. Degradable, pH-sensitive, membrane-destabilizing, comb-like polymers for intracellular delivery of nucleic acids. Biomaterials. 2010; 31(27):7150–7166. [PubMed: 20579726]
29. Morris MC, Depollier J, Mery J, Heitz F, Divita G. A peptide carrier for the delivery of biologically active proteins into mammalian cells. Nat Biotechnol. 2001; 19(12):1173–1176. [PubMed: 11731788]
30. Lackey CA, Press OW, Hoffman AS, Stayton PS. A biomimetic pH-responsive polymer directs endosomal release and intracellular delivery of an endocytosed antibody complex. Bioconjugate Chem. 2002; 13(5):996–1001.
31. Berthiaume EP, Medina C, Swanson JA. Molecular size - fractionation during endocytosis in macrophages. Journal of Cell Biology. 1995; 129(4):989–998. [PubMed: 7538141]
32. Dunn WA, Hubbard AL, Aronson NN. Low-Temperature Selectively Inhibits Fusion between Pinocytic Vesicles and Lysosomes during Heterophagy of Asialofetuin-I-125 by the Perfused-Rat-Liver. J Biol Chem. 1980; 255(12):5971–5978. [PubMed: 6155379]
33. Liu JM, Xiao NQ, DeFranco DB. Use of digitonin-permeabilized cells in studies of steroid receptor subnuclear trafficking. Methods. 1999; 19(3):403–409. [PubMed: 10579935]
34. Korn ED. Cell Membranes - Structure and Synthesis. Annu Rev Biochem. 1969; 38 263-&.
35. Schutt F, Bergmann M, Holz FG, Kopitz J. Isolation of intact lysosomes from human RPE cells and effects of A2-E on the integrity of the lysosomal and other cellular membranes. Graef Arch Clin Exp. 2002; 240(12):983–988.
36. Seksek O, Biwersi J, Verkman AS. Translational diffusion of macromolecule-sized solutes in cytoplasm and nucleus. Journal of Cell Biology. 1997; 138(1):131–142. [PubMed: 9214387]
37. Johansson A-C, Appelqvist H, Nilsson C, Kagedal K, Roberg K, Ollinger K. Regulation of apoptosis-associated lysosomal membrane permeabilization. Apoptosis. 2010; 15(5):527–540. [PubMed: 20077016]
38. Tran, K. Department of Chemical Engineering. University of Washington; 2011. Engineering Immunity Through the Rational Design of Vaccines.
39. Manganiello MJ, Cheng C, Convertine AJ, Bryers JD, Stayton PS. Diblock copolymers with tunable pH transitions for gene delivery. Biomaterials. 2012; 33(7):2301–2309. [PubMed: 22169826]
40. Behr JP. The proton sponge: A trick to enter cells the viruses did not exploit. Chimia. 1997; 51(1–2):34–36.

Author Manuscript Author Manuscript Author Manuscript Author Manuscript

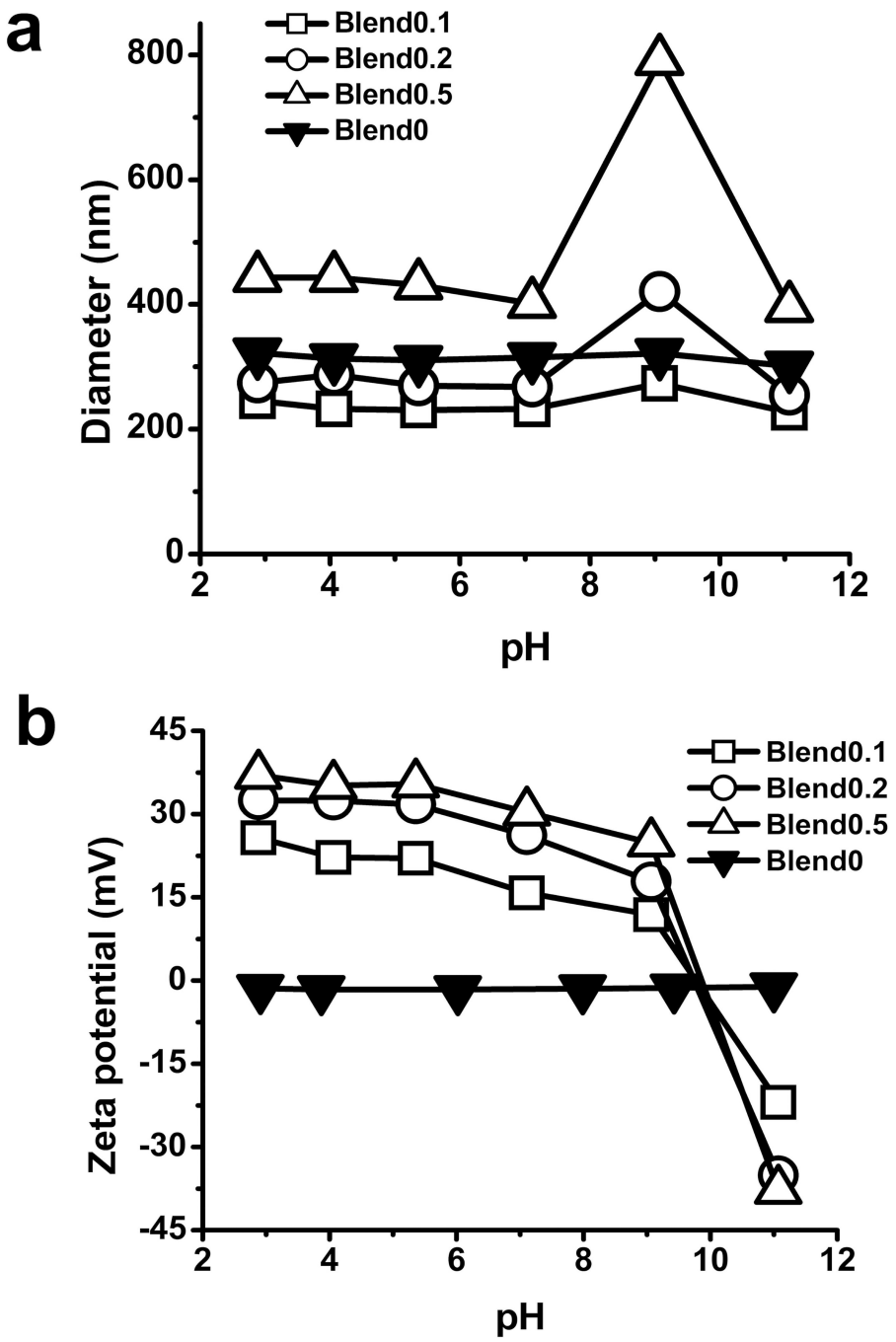

Fig 1. Characterization of blend particles by DLS

The hydrodynamic diameters (a) and zeta potential (b) of blend particles determined by DLS. Size and zeta potential of blend particles were measured in a 10 mM KNO3 solution with pH ranging from 2 to 12. Values are the mean size or zeta potential of particles from three independent batches ± S.E.

Author Manuscript
Author Manuscript
Author Manuscript
Author Manuscript

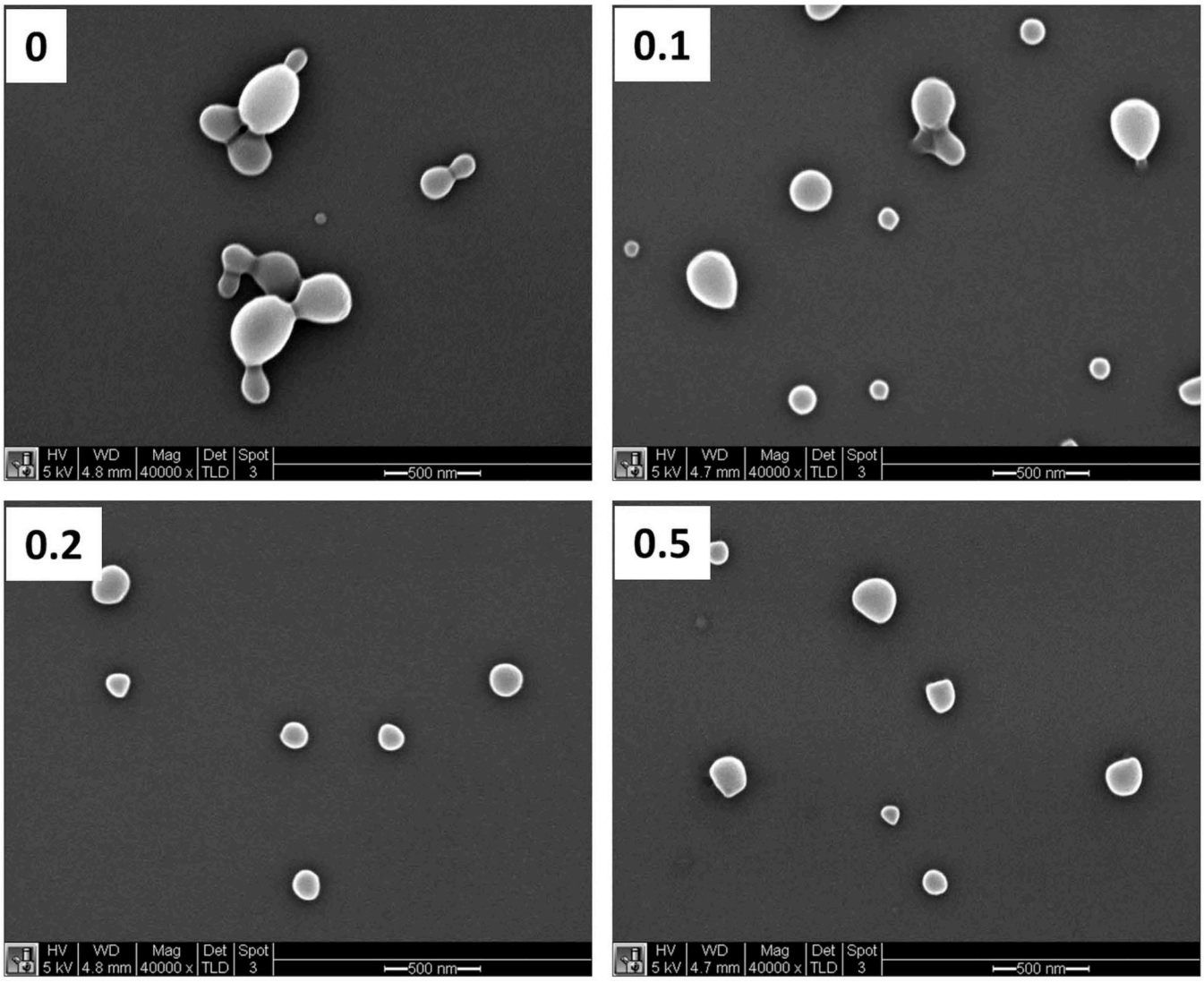

Fig 2. Characterization of blend particles by scanning electron microscopy (SEM)

SEM micrographs of the blend particles with 0, 0.1, 0.2 or 0.5 weight fraction of BMA-DMAEMAPAA tripolymer, respectively. Scale bar=500 nm.

Author Manuscript Author Manuscript Author Manuscript Author Manuscript

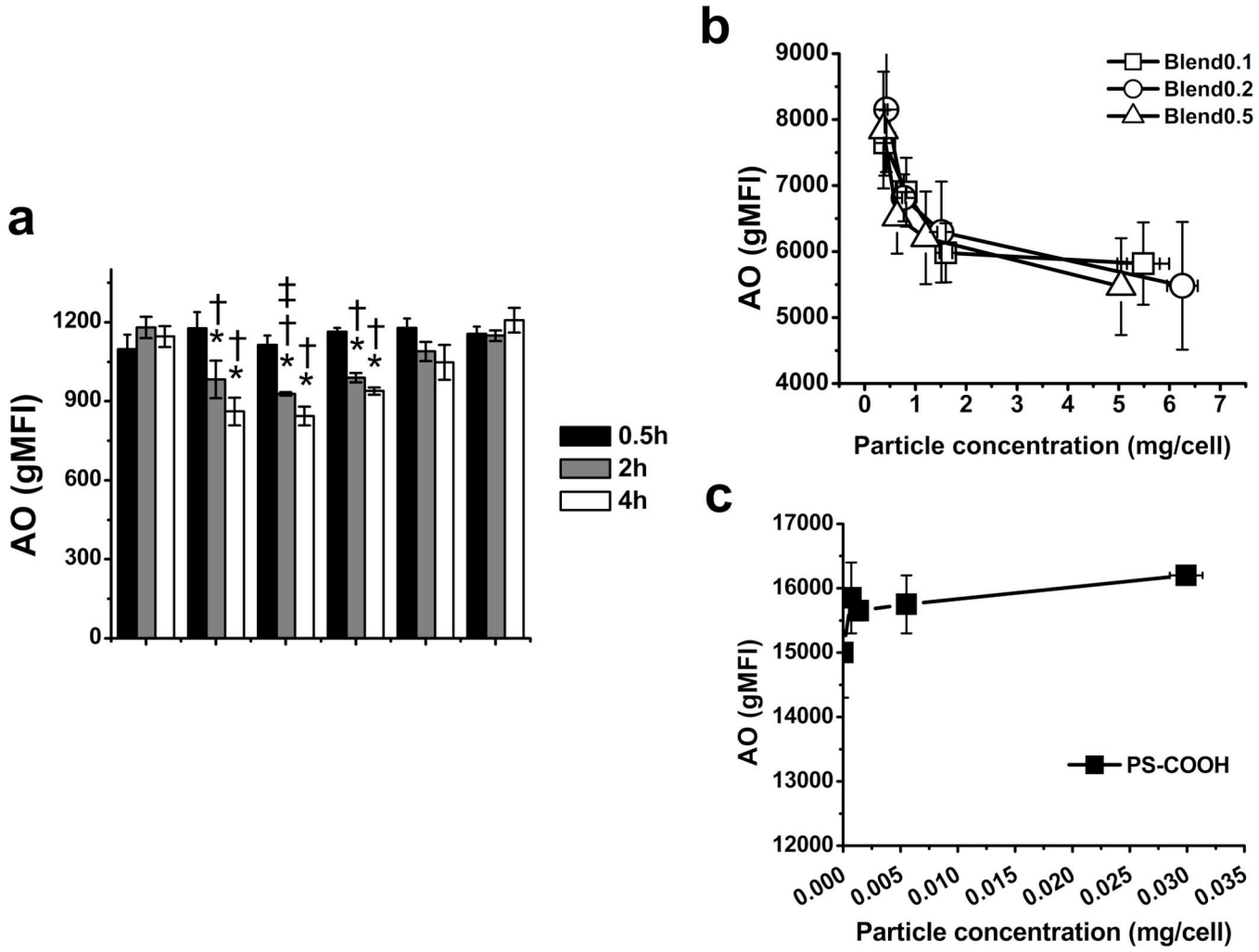

Fig 3. Endosomal escape mediated by blend particles assessed by acridine orange (AO)

The fluorescent intensity change of AO at 640 nm in DC2.4 cells in the presence of blend particles and polystyrene (PS) particles at different incubation times (a) and particle concentrations (b) and (c). PS-NH2 and PS-COOH indicate the amine-modified and carboxylate-modified polystyrene particles with 200 nm in diameter, respectively. The values are mean ± S.E. Asterisk, dagger and double dagger indicate $p < 0.05$ with respect to the medium control, PS-COOH and PS-NH2 groups of DC2.4 cell, respectively.

Author Manuscript Author Manuscript Author Manuscript Author Manuscript

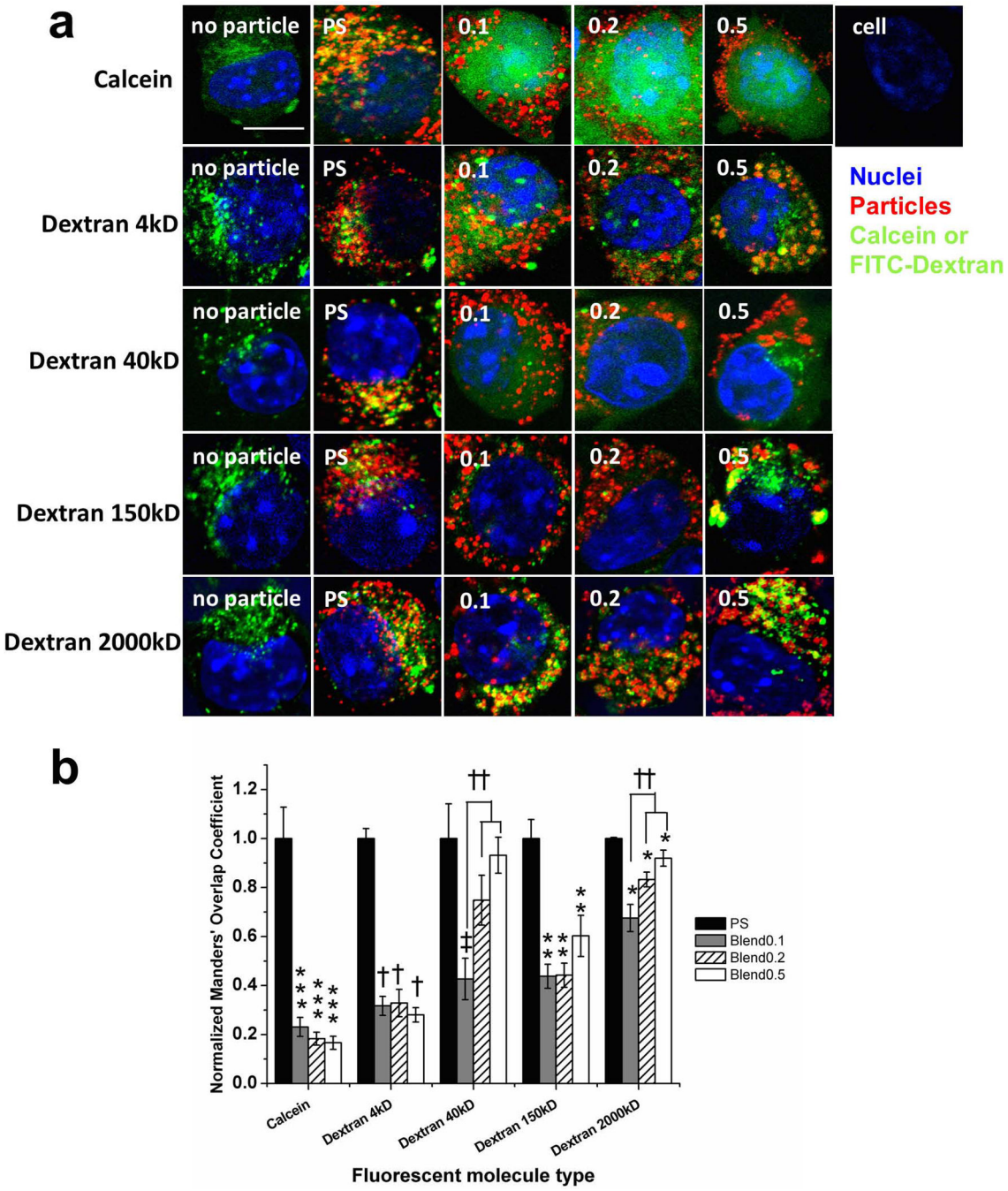

Fig 4. Confocal microscopic analysis of the intracellular distribution of calcein and FITC-dextran with different molecular weights (4, 40, 150 and 2,000 k Da) in DC2.4 cells

Calcein and FITC-dextran molecules were co-delivered with blend particles or PS particles (a). 4 h later, cells were washed and fixed for confocoal microscopic analysis. PS represents the carboxylate-modified polystyrene beads (200 nm). Blue: nucleus, green: calcein or FITC-dextran, red: particles. Scale bar = 10 μm. The images are representative of two independent experiments. Three to five regions for each sample were taken by confocal microscopy at 63 × oil immersion. Manders' coefficient of fluorecent cargo for different types of particles (b). ImageJ and a plug-in JACoB were utilized for computing co-

Author Manuscript Author Manuscript Author Manuscript Author Manuscript

localization coefficients (Manders'). Fifteen cells for each group were chosen and the Manders' coefficient of fluorescent cargo was plotted. The values are mean ± S.E, and normalized to the value of polystyrene particle (PS) in each fluorescent cargo group. Asterisks, double asterisks, triple asterisks, daggesr and double daggers indicate $p < 0.05$ respect to the each PS sample.

Author Manuscript Author Manuscript Author Manuscript Author Manuscript

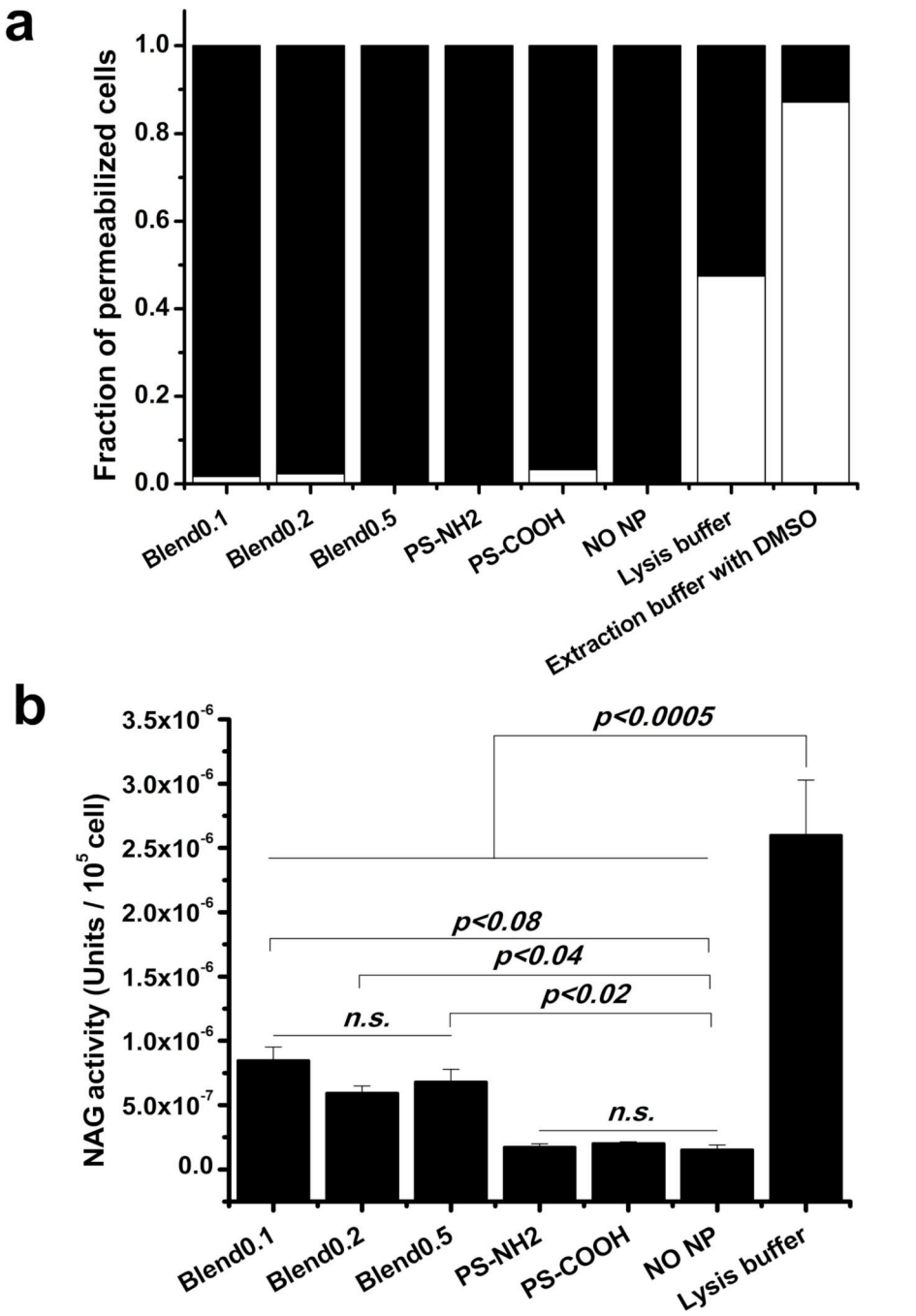

Fig 5. The release of lysosomal enzyme, N-acetyl-β-D-glucosaminidase (NAG), mediated by blend particles

DC2.4 cells were exposed to blend particles or PS particles for 4 h at 37°C, and then treated with digitonin. The fraction of permeabilized cells assessed by trypanblue staining for each cell types (blend0.1, blend0.2, blend0.5, PS-NH2, PS-COOH) (a). Black: permeabilized cells; white: membrane-intact cells. Cytosol NAG activity was measured with β-N-Acetylglucosaminidase assay kit and expressed as enzyme units per 10^5 permeabilized cells (b).

Author Manuscript

Author Manuscript

Author Manuscript

Author Manuscript

Table 1

Characterization of blend particles by NMR

Particle name	Tripolymer used in fabrication (wt fraction)	BMA hydrogen: glycolide ratio (from NMR spectra)	Actual terpolymer in particle (wt fraction)
Blend 0	0	0	0
Blend 0.1	0.1	0.0712	0.112
Blend 0.2	0.2	0.1524	0.240
Blend 0.5	0.5	0.3633	0.420

Author Manuscript

Author Manuscript

Author Manuscript

Author Manuscript

Table 2

The diameter of particles obtained by DLS or SEM

DLS (pH 6)	Blend0	Blend0.1	Blend0.2	Blend0.5
size(nm)	310.07	230.7	269.4	430.87
PDI	0.1227	0.0817	0.094	0.1133
zeta(mV)	−1.6267	22.03	31.73	35.40
SEM	**Blend0**	**Blend0.1**	**Blend0.2**	**Blend0.5**
size(nm)	188.03 ± 6.69	192.87 ± 5.85	170.97 ± 3.71	146.89 ± 3.73